Electronic Supplementary Information

Radiation-Hard Organic Electronics *via* Perylenediimide Core Engineering

Sergey A. Kuklin,[a] Petr M. Kuznetsov,[a] Valeria S. Bolshakova,[a] Gennady V. Shilov,[a] Alexander V. Mumyatov,[a] Mikhail V. Zhidkov,[a] Galina A. Kichigina,[a] Pavel P. Kushch,[a] Evgeny V. Golosov,[a] Dmitry P. Kiryukhin,[a] and Pavel A. Troshin*[b,a]

[a] *Federal Research Center for Problems of Chemical Physics and Medicinal Chemistry RAS, Academician Semenov ave. 1, Chernogolovka, 142432, Russia*

[b] *Zhengzhou Research Institute of HIT, Longyuan East 7th, 26, Jinshui District, 450003 Zhengzhou, China*

Contents:

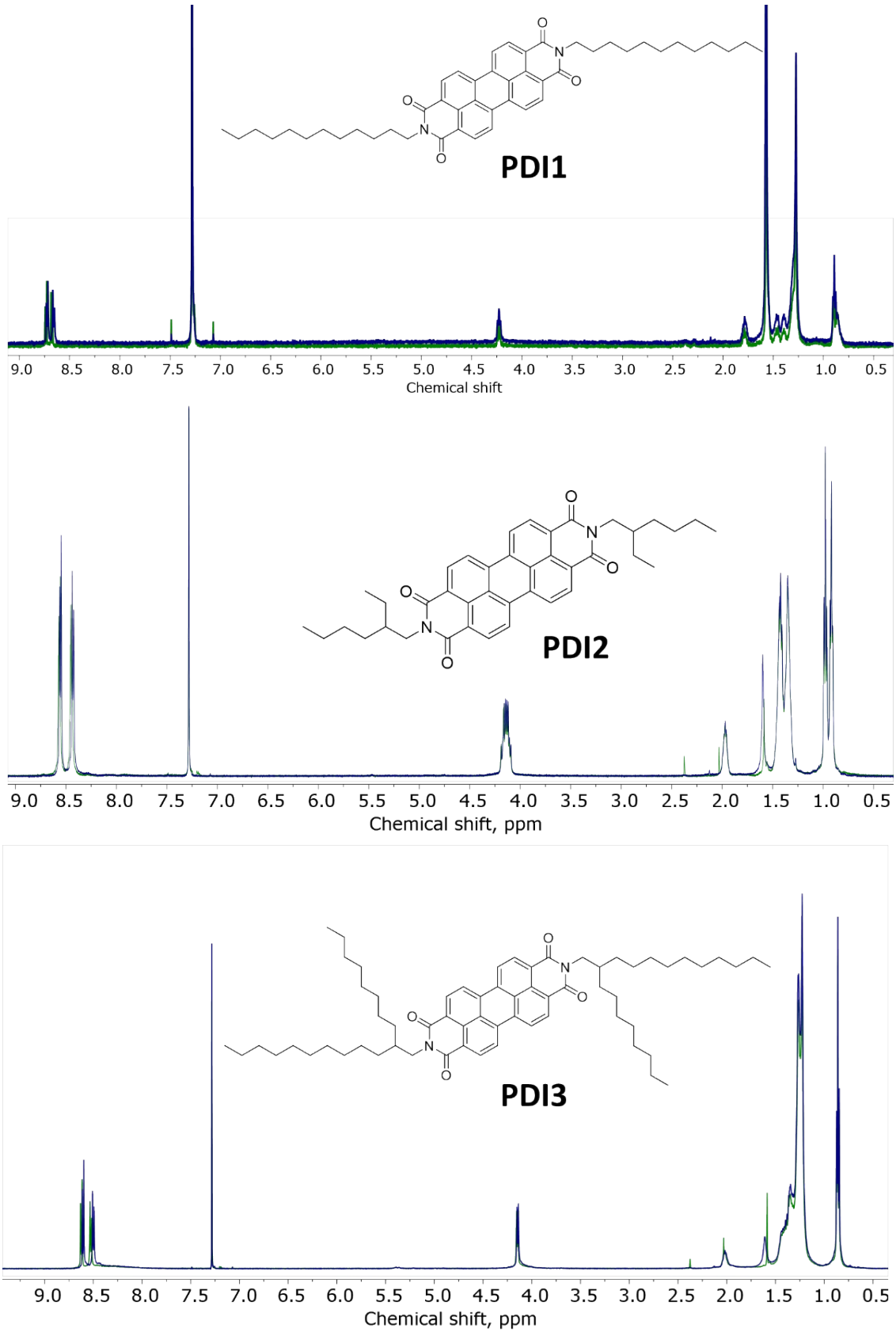

Figure S1. ^{1}H NMR spectra of **PDI1-3** before (green) and after (blue) exposure to 8.0 MGy of gamma rays.

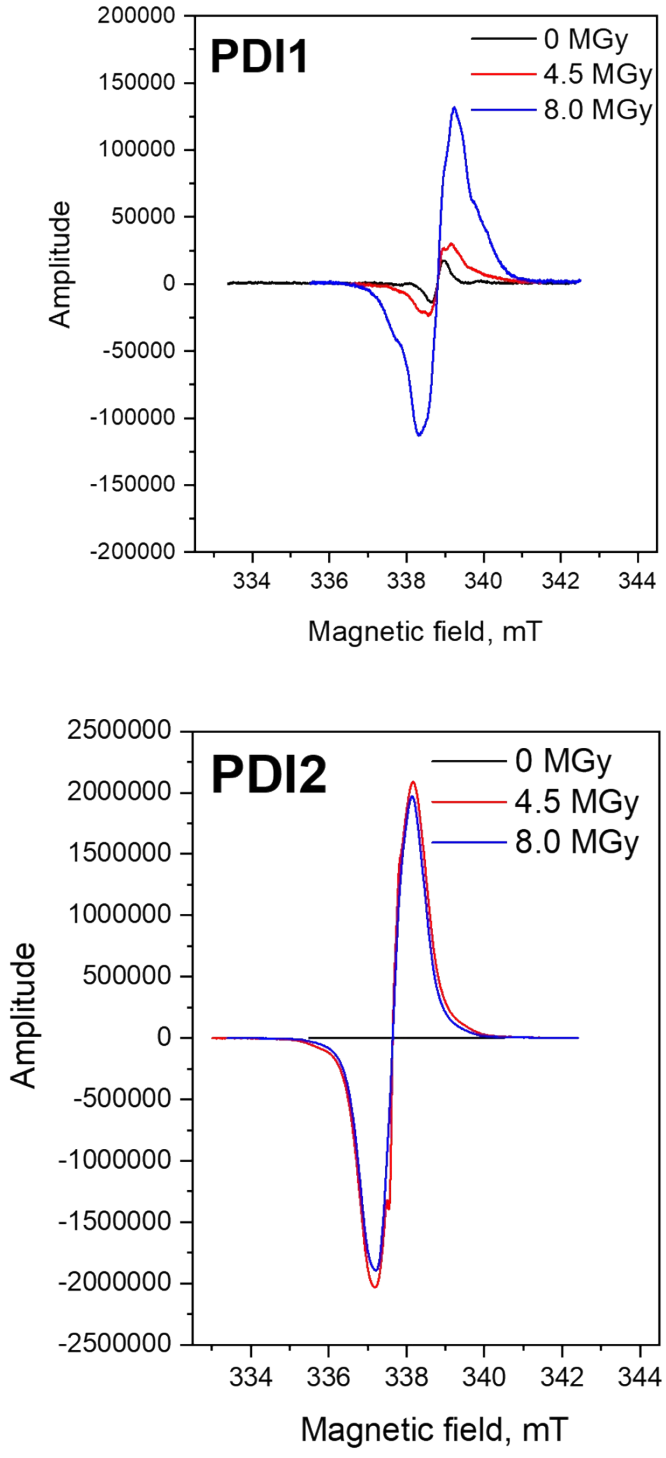

Figure S2. ESR spectra of **PDI1** and **PDI2** before and after exposure to 4.5 and 8.0 MGy of gamma rays.

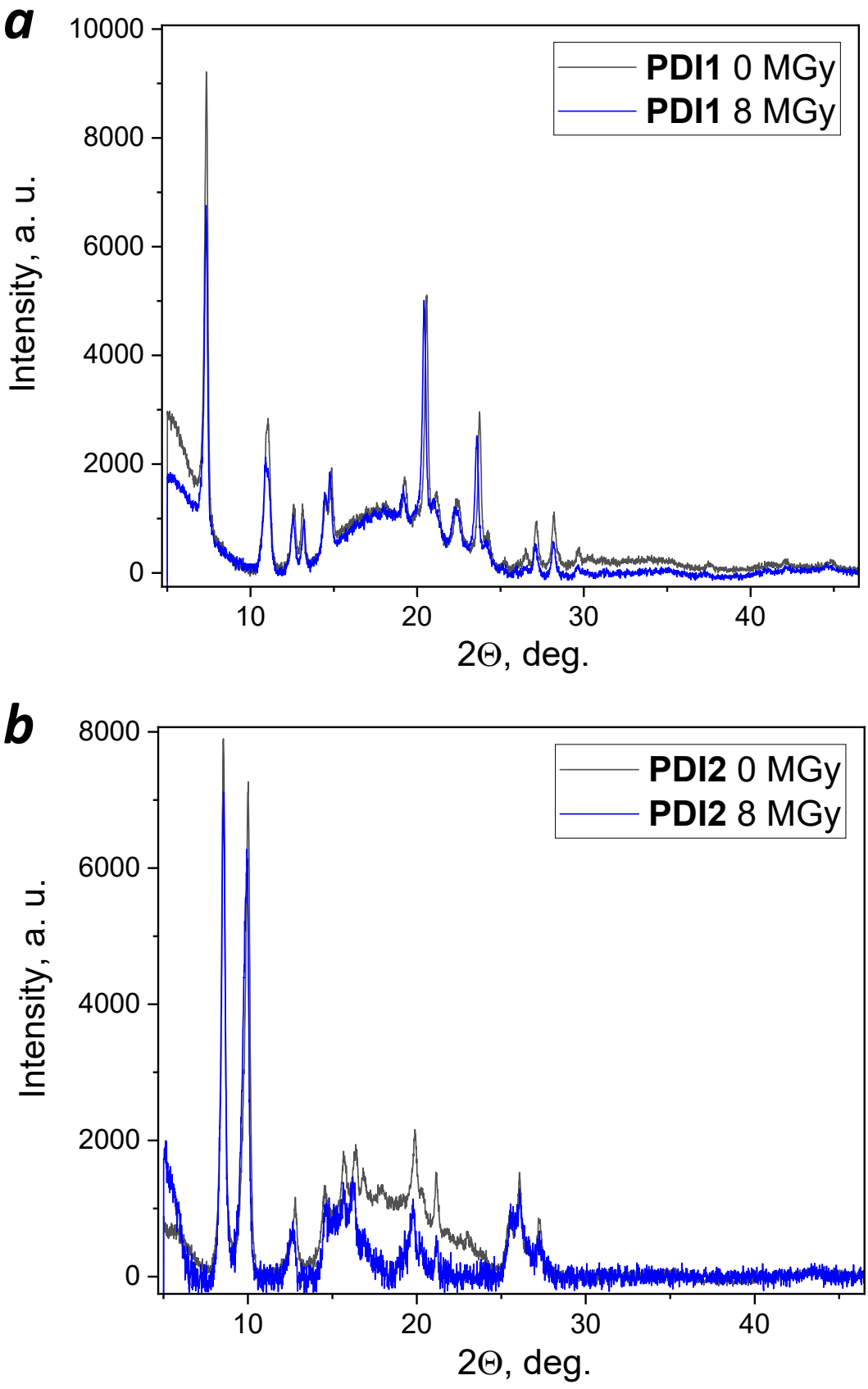

Figure S3. XRD patterns of **PDI1** and **PDI2** powders before and after exposure to 8.0 MGy of gamma rays.

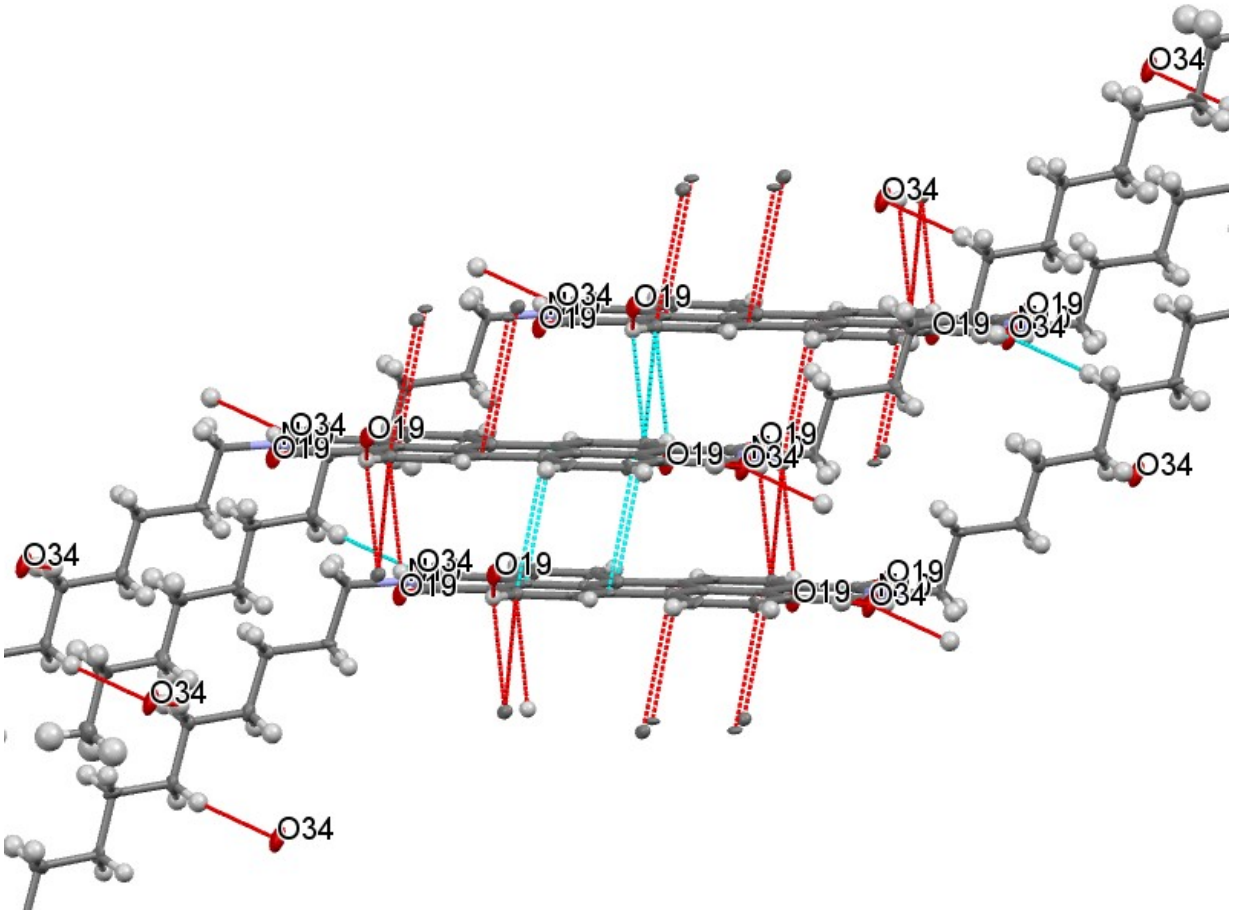

Figure S4. Packing of the molecules in the crystal structure of **PDI1**

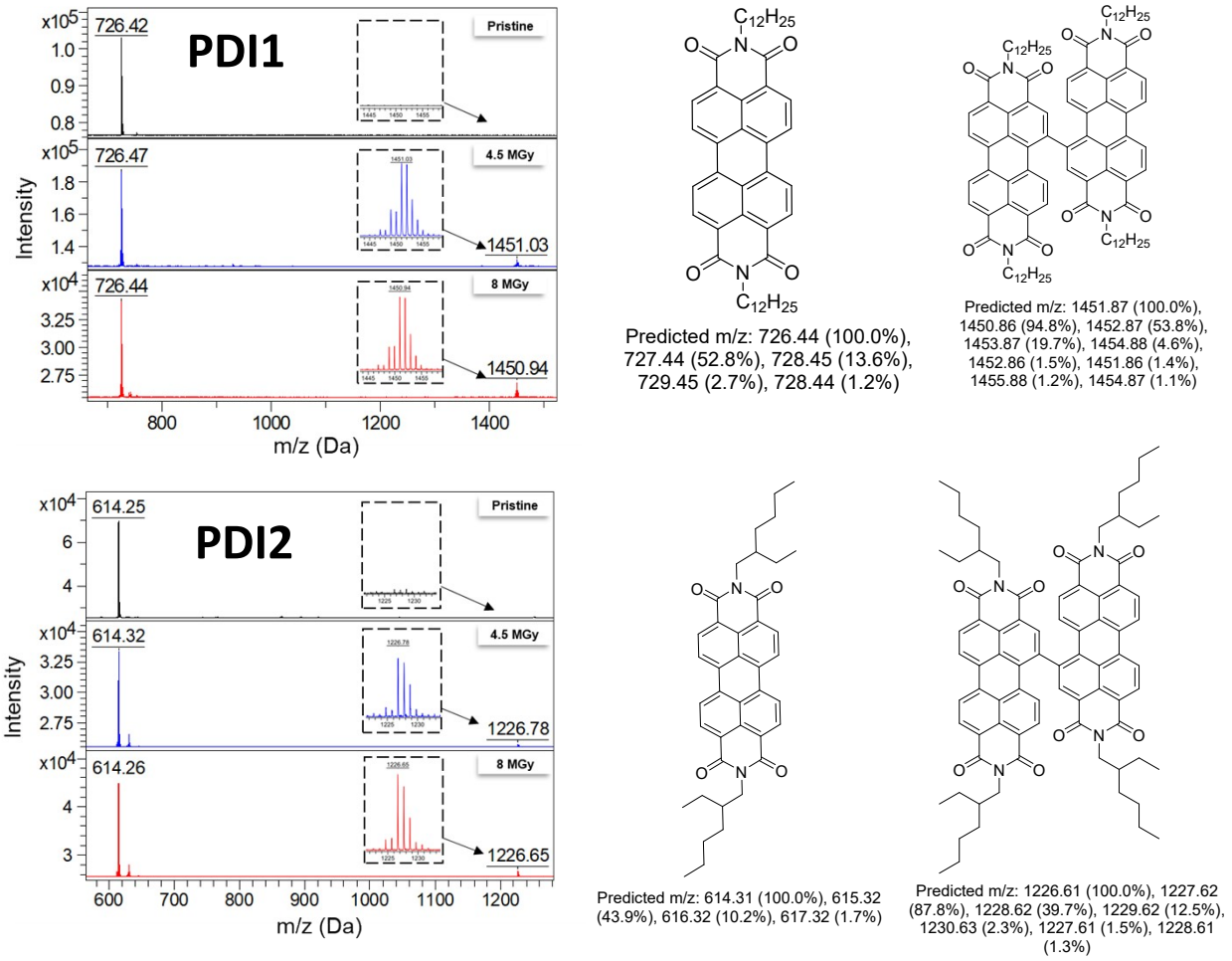

Figure S5. MALDI ToF mass spectra of **PDI1** and **PDI2** before and after exposure to 4.5 and 8.0 MGy of gamma rays. Predicted m/z values for the corresponding monomeric and dimeric species are given on the right side

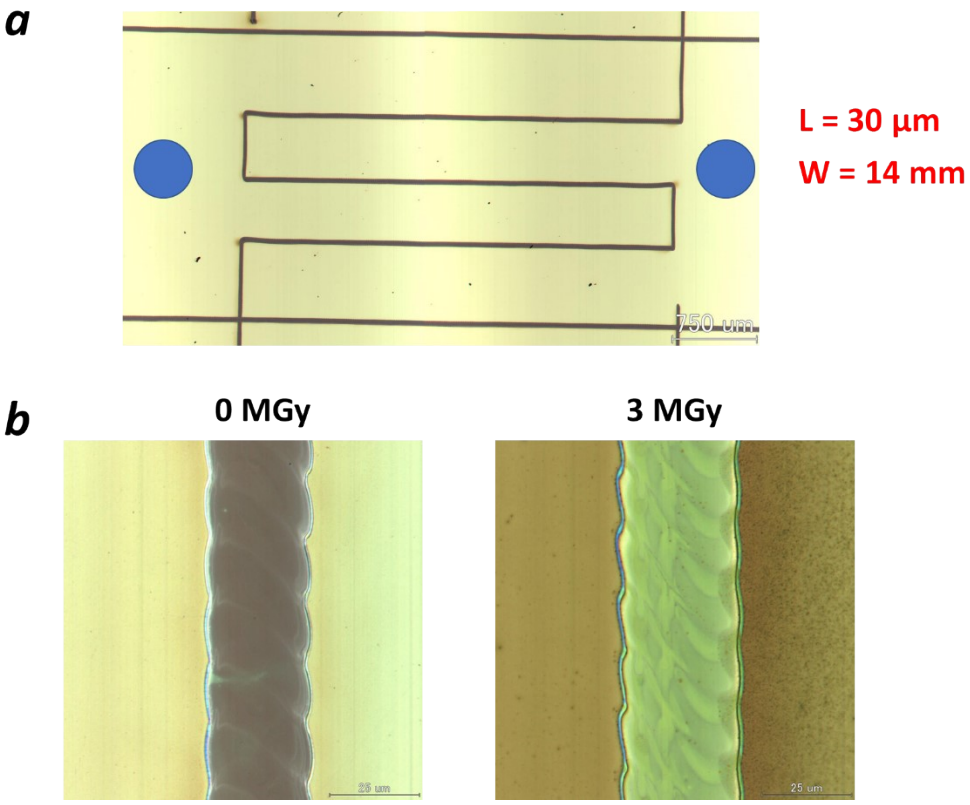

Figure S6. Confocal optical microscopy image of the lateral resistor device prepared by laser patterning of ITO on glass. Two blue circles indicate positions of the probes during the measurements (a). Magnified microscopy images of the device channel with **PDI5** as semiconductor obtained before and after exposure to 3 MGy of gamma rays.

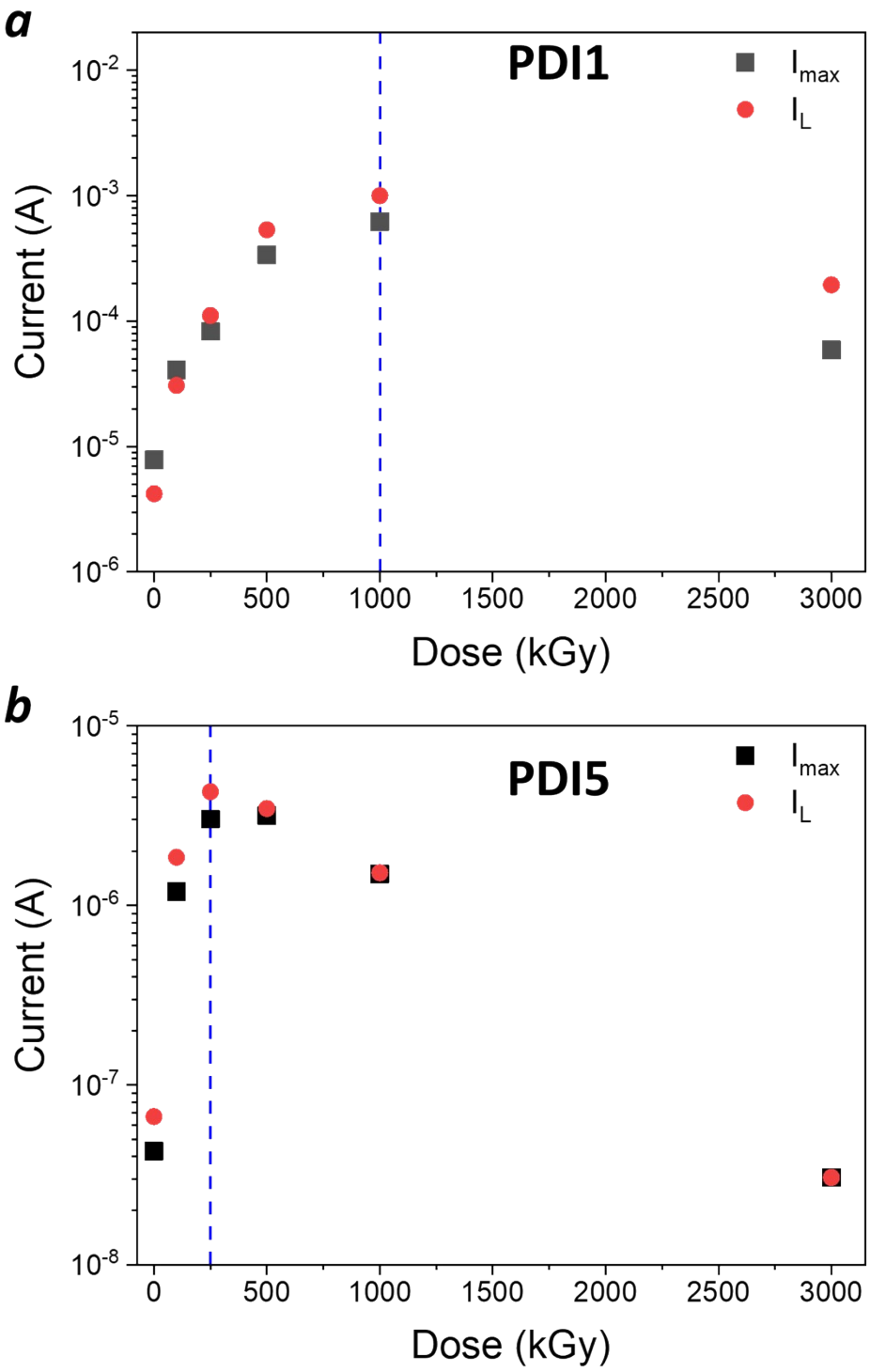

Figure S7. Radiation hardness assessment for photoresistors based on **PDI1** (a) and **PDI5** (b). The radiation dose dependences of the light current I_L from the stationary I-V measurements (at 200 V) and maximum peak current I_{max} from the dynamic photoresponse measurements (when light pulse is detected). Blue dashed lines represent the guide for the eye showing schematically stability thresholds for different materials.

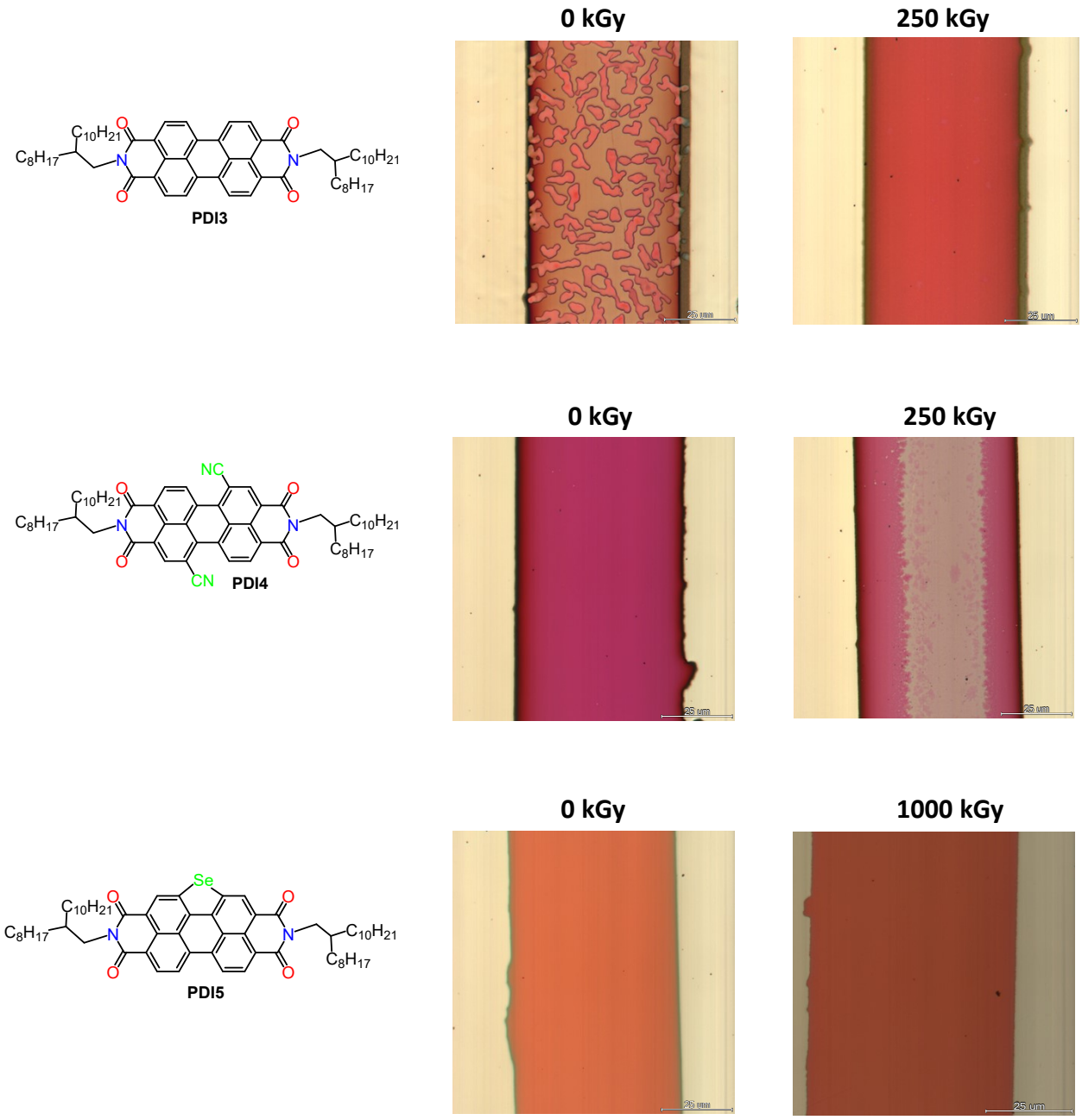

Figure S8. Confocal optical microscopy images of the OFET channels with different PDI-based semiconductors before and after radiation exposure.

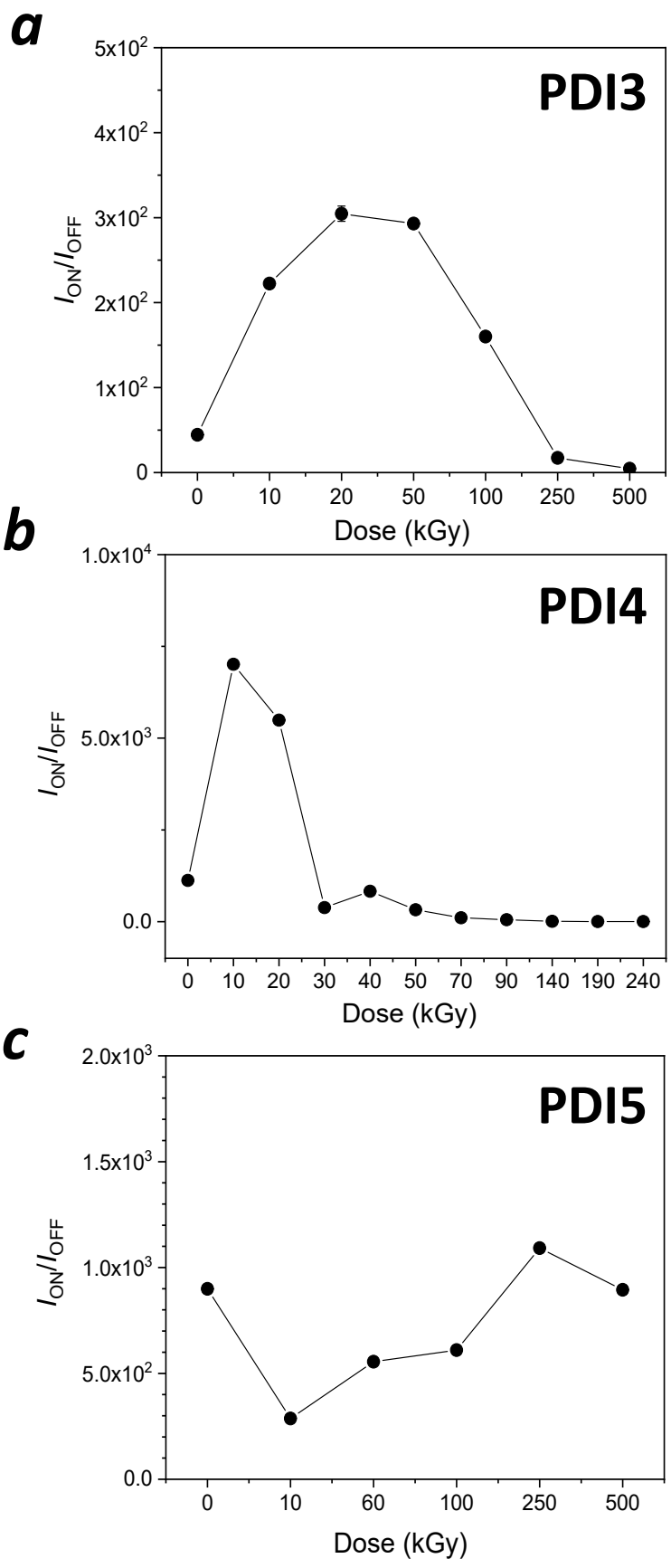

Figure S9. Radiation dose dependences for the I_{ON}/I_{OFF} current ratios in OFETs based on **PDI3** (a), **PDI4** (b), and **PDI5** (c)

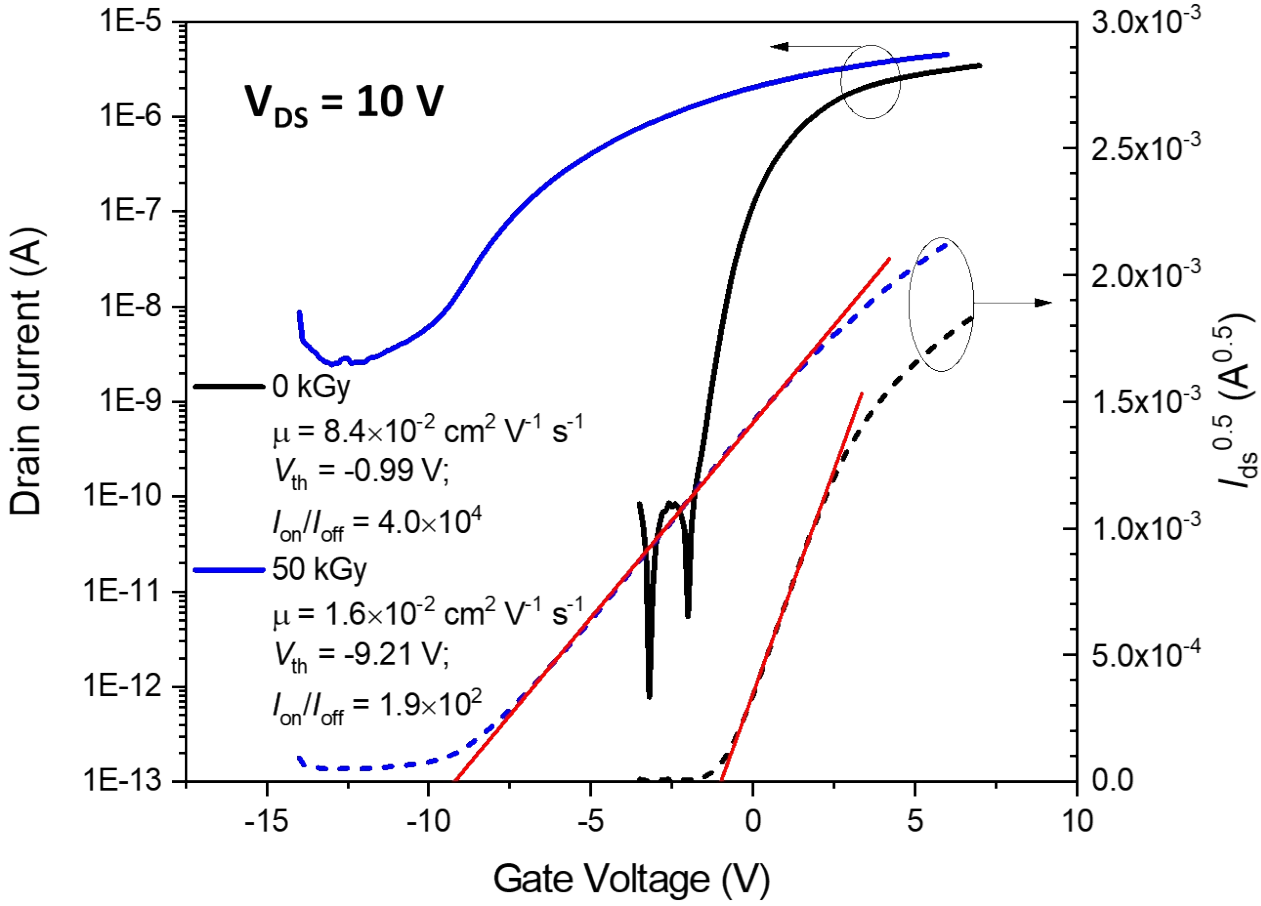

Figure S10. Transfer characteristics and $I_{DS}^{1/2}$ vs. V_{GS} plots for champion OFETs with **PDI4** semiconductor layer before and after exposure to 50 kGy of gamma rays.

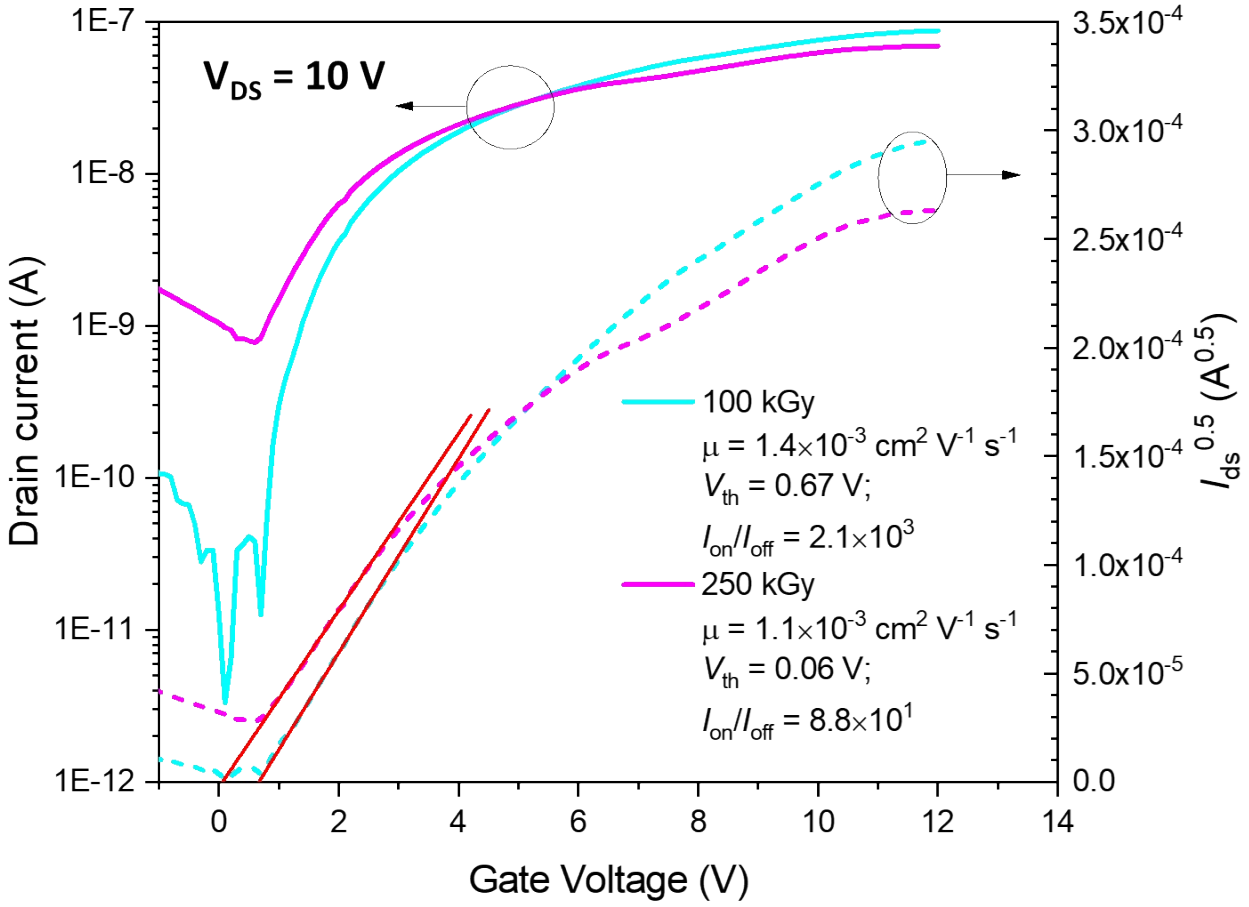

Figure S11. Transfer characteristics and $I_{DS}^{1/2}$ vs. V_{GS} plots for champion OFETs with **PDI3** semiconductor layer after exposure to 100 and 250 kGy of gamma rays.

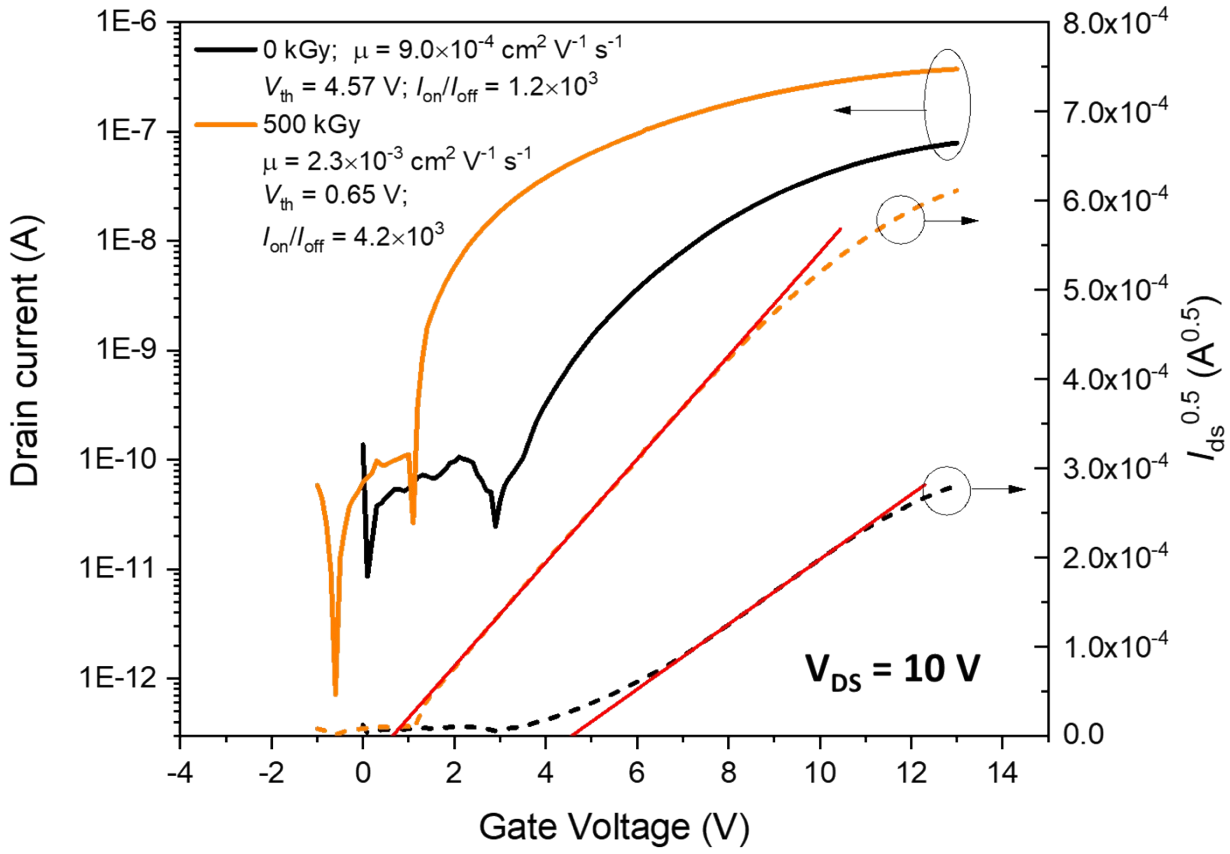

Figure S12. Transfer characteristics and $I_{DS}^{1/2}$ vs. V_{GS} plots for champion OFETs with **PDI5** semiconductor layer before and after exposure to 500 kGy of gamma rays.

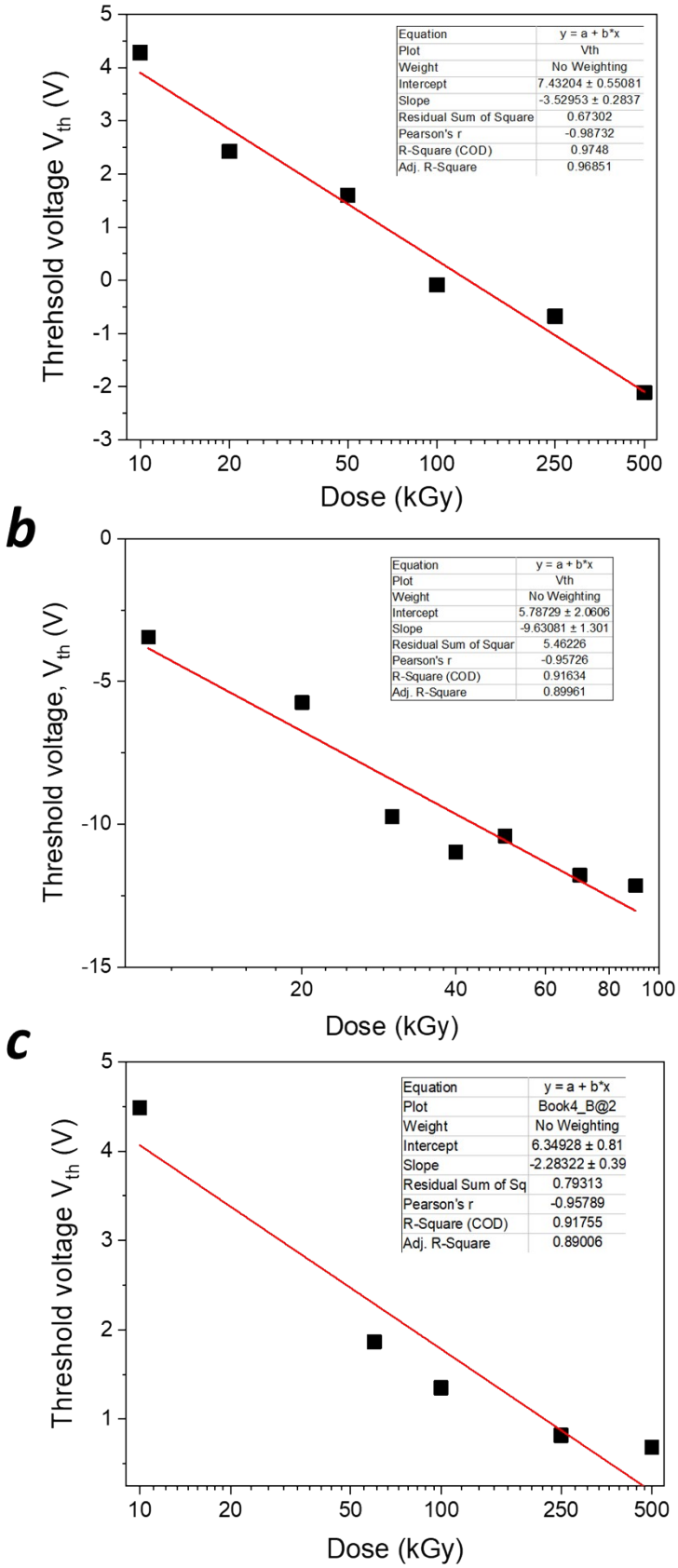

Figure S13. Dose-dependent evolution of the threshold voltages in OFETs based on **PDI3** (a), **PDI4** (b), and **PDI5** semiconductor layers plotted in semilogarithmic scale

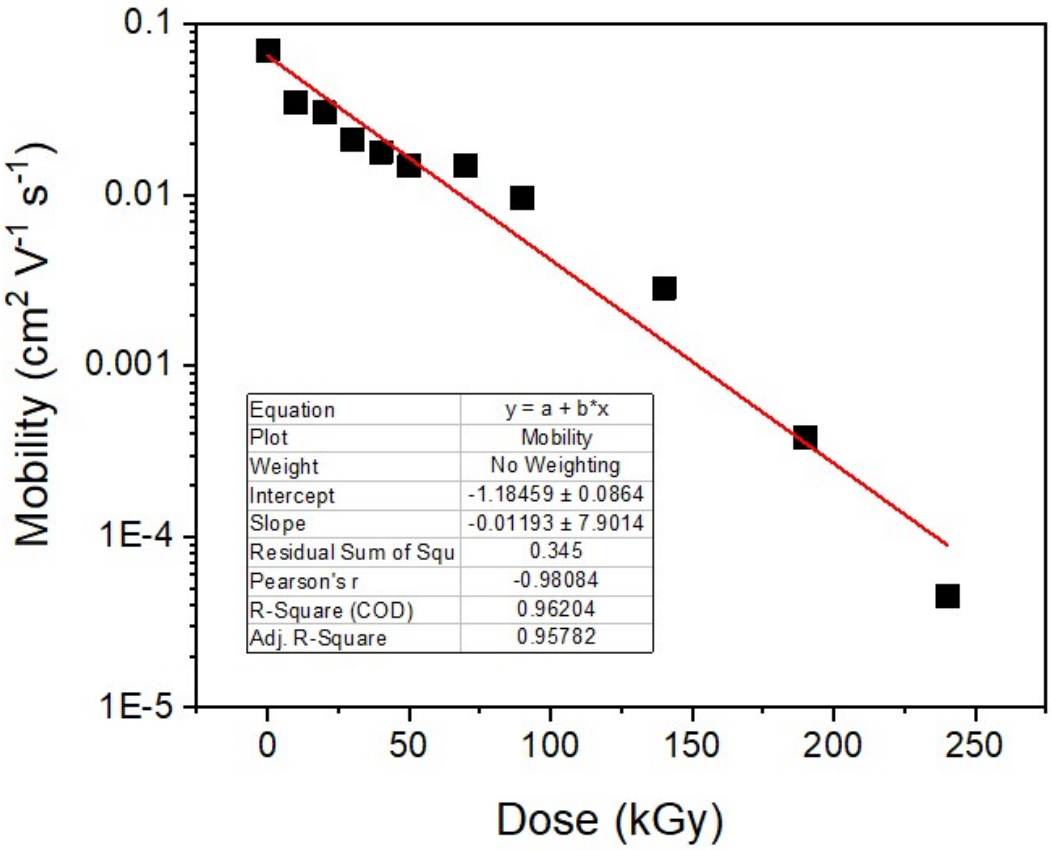

Figure S14. Dose-dependent evolution of the charge carrier mobility in OFETs based on **PDI4** plotted in semilogarithmic scale